

## LHAASO detection of the Gamma-ray Emission from the W43 Direction

---

**Guangwei Wang,<sup>a,c,\*</sup> Chuandong Gao<sup>b,c</sup> and Ruizhi Yang<sup>a</sup> on behalf of the LHAASO collaboration**

<sup>a</sup>*University of science and technology of china, Department of astronomy, 230026 Hefei, Anhui, China*

<sup>b</sup>*Institute of Frontier and Interdisciplinary Science, Shandong University 266237 Qingdao, Shandong, China*

<sup>c</sup>*Key Laboratory of Particle Astrophysics, Institute of High Energy Physics, Chinese Academy of Sciences 100049 Beijing, China*

*E-mail: [wanguangwei@mail.ustc.edu.cn](mailto:wanguangwei@mail.ustc.edu.cn), [gaocd@ihep.ac.cn](mailto:gaocd@ihep.ac.cn), [yangrz@ustc.edu.cn](mailto:yangrz@ustc.edu.cn)*

We report the very-high-energy to ultra-high-energy  $\gamma$ -ray emission, detected by the Large High Altitude Air Shower Observation (LHAASO), from the direction toward the young star forming region W43. The extended  $\gamma$ -ray source is detected with a significance of  $\sim 19\sigma$  with KM2A and a significance of  $\sim 17\sigma$  with WCDA.

38th International Cosmic Ray Conference (ICRC2023)  
26 July - 3 August, 2023  
Nagoya, Japan



---

\*Speaker

## 1. Introduction

W43 is a giant HII region in the inner Galaxy. It is located at the connection points between the Galactic bar and the Scutum-Centaurus arm, where gas collisions may be particularly intense, featuring complex gas dynamics. Due to its extremely high star formation rate, it is a Galactic mini star-burst, which contributes about 5% – 10% of the total star formation rate in the whole Galaxy [1, 2]. The center of W43, W43-main, is a huge HII region excited by a Wolf-Rayet and OB star cluster.

The origin of Galactic cosmic rays is one of the most important puzzles in astronomy. By observing  $\gamma$ -ray emissions, we can indirectly study the origins of cosmic rays, their interactions with the surrounding gaseous and magnetic environments, and their propagation through these environments. Stellar winds from massive stars are one possible origin of cosmic rays [3]. Therefore, W43 is an ideal region for studying the origins of cosmic rays in star-forming areas. Furthermore,  $\gamma$ -ray emissions have also been detected in this region, possibly closely linked to the cosmic ray activities that may be present in the region. An extended TeV source has also been detected by H.E.S.S telescope [4]. Abramowski et.al [5] also found GeV excess in this region and attribute that to a potential PWN, but the powering pulsar is not found yet. Recently, Yang et.al [6] has found an extended  $\gamma$ -ray emissions in this region with a radius of about  $0.6^\circ$  with a significance of 16. They derived a hard  $\gamma$ -ray spectrum with a spectral index of about 2.3. The large extension with a physical size of about 50pc and the hard  $\gamma$ -ray spectrum is very similar to other  $\gamma$ -ray bright young massive clusters in our Galaxy [7]. In this scenario, the  $\gamma$ -ray emissions in the vicinity of W43 are produced by the interaction of cosmic rays injected by W43 interacting with ambient gas, through the pion-decay process. And W43 is believed to harbor cosmic ray accelerators.

LLHAASO [8] discovered the first 12 ultra-high-energy  $\gamma$ -ray sources in the Galactic plane. One of them, LHAASO J1849-0003, is spatially close to W43. In the first  $\gamma$ -ray source catalog released recently by LHAASO collaboration [9], the ultra-high-energy source is further resolved into several sources, in which 1LHAASO J1848-0153u which is a ultra-high-energy source spatially coincides with the GeV emissions in W43. Thus a natural postulation is that W43 can even be a PeV cosmic ray accelerator.

In this paper, we performed a preliminary data analysis using LHAASO KM2A and WCDA data on W43 region. Thanks to the accumulated exposure and better understanding of the response of the instruments we have a much more significant detection. This paper is organized as follows, in Sec.2 we described the LHAASO data analysis taking into account both WCDA and KM2A array, in Sec.3 we show the preliminary result, in Sec.4 we discussion the multi wavelength observation.

## 2. LHAASO data analysis

The Large High Altitude Air Shower Observation (LHAASO), located at Haizi Mountain, Daocheng, Sichuan province, China, is composed three subarrays, including the  $1\text{km}^2$  array (KM2A), the Water Cherenkov Detector Array (WCDA), and the WideField air Cherenkov/fluorescence Telescopes Array (WFCTA). One of the most important scientific goals of LHAASO is searching the origin of the cosmic rays in our galaxy.

In our analysis, the low-energy gamma-ray data ( $E < 25\text{TeV}$ ) were collected by the whole WCDA, covering an area of 78000 m<sup>2</sup>, from 100GeV to 20TeV [10]. The data used in this study were obtained from the full-array operation of the WCDA from March 5, 2021 to September 30, 2022, with a total exposure time of 506 days. To select events, the Gamma-Proton identification parameter called "pinncness" was set to be less than 1.1, and the zenith angle of the shower was required to be less than 50 degrees. The data were divided into five energy segments based on the number of triggered detectors (nhit), with ranges of 100-200, 200-300, 300-500, 500-800, and 800-2000. The medium energy of events with nhit greater than 100 is approximately 2 TeV, with a power-law spectrum index of -2.6. For each energy segment, the sky map in celestial coordinates (right ascension and declination) is divided into a grid of  $0.1^\circ \times 0.1^\circ$  each pixel which is filled with the number of the detected events according to their reconstructed arrival direction. The cosmic ray background was estimated using the "Time-Swap" method [11].

The high-energy gamma-ray data ( $E > 25\text{TeV}$ ) were collected by KM2A. KM2A is a unique array focusing on detection of very-high-energy and ultra-high-energy sources in the northern sky. KM2A covers an area of 1km<sup>2</sup>, it is composed of two different parts: 4911 electric detectors which can detect charged particles in the extensive air shower and 1188 muon detectors which can detect muons in the extensive air shower and significantly reduce the background of cosmic rays in gamma-ray observations. The data were collected from different phases of the KM2A array: half the array since December 2019 to December 2020, three-quarters of the array from December 2020 to July 2021, and the full KM2A array from July 2021 to April 2023. The total effective observation time is 1124.28 days for KM2A after the data quality check. The selection criteria for the events used for this work is:

- $0^\circ < \text{zenith} < 50^\circ$
- $N_{pE1} > 10 \ \&\& \ N_{filtE} > 10 \ \&\& \ N_{hitM} > 10 \ \&\& \ N_{trigE} > 19$
- $N_{pE1}/N_{pE2} > 2$
- $dr > 20\text{m}$  (for half array  $dr > 0\text{m}$ )
- $0.6 < \text{age} < 2.4$

For gamma ray/background discrimination, we used the ratio  $R = \log((N_u + 0.0001)/N_e)$  as an indicator. The R for each energy bin is -5.11, -5.24, -5.95, -6.08, -2.34, -2.35, -2.36, -2.36, -2.36, -2.36, -2.36, -2.36, respectively. The KM2A data sets are divided into five groups per decade according to the reconstructed energy upon to 4 PeV. For the data set in each group, the celestial coordinates (right ascension and declination) is also divided into a grid of  $0.1^\circ \times 0.1^\circ$  each pixel and filled detected events according to their arrival direction. The "direct integration method" [11] was used to estimate the residual cosmic-ray background after  $\gamma$ -ray /background discrimination.

In this work, we used binned likelihood method to find new sources or determine the spectrum and morphology of sources. In binned likelihood method, to compare the goodness of each hypothesis, the Test Statistic  $TS = 2 \log(\lambda)$  is used, where  $\lambda = \mathcal{L}_1/\mathcal{L}_0$ ,  $\mathcal{L}_1$  is the maximum likelihood value for the alternative hypothesis, which we may want to prove, while  $\mathcal{L}_0$  is the maximum likelihood value of the null hypothesis. According to Wilks' Theorem[12], the TS value

follows a chi-square distribution whose number of degrees of freedom is the difference between the numbers of free parameters in the null hypothesis and the alternative hypothesis. Therefore, if the TS value is larger, the alternative hypothesis is more credible than the null hypothesis.

To check for the presence of additional sources and to obtain the morphology or significance distribution of the observed sources, we generated significance sky maps using the maximum likelihood method. We conducted a hypothesis test at the center of each position bin. The null hypothesis is there is only background in the ROI, while the alternative hypothesis is there is an additional point source in the test position. In the following analysis, the point source is assumed to have a power-law spectrum with a fixed spectral index and a variable parameter of flux. For KM2A data, the spectrum index is assumed to be 3.0. For WCDA data, the spectrum index is assumed to be 2.6. Thus,  $\pm\sqrt{\text{TS}}$  is actually the significance of the alternative hypothesis, according to the Wilks' theorem. If the TS value is larger than 25. If the TS value is greater than 25, or equivalently, the significance is greater than 5, it suggests that there might be a signal excess at this location. The morphology of the significance distribution can also reflect the morphology of the source.

An iterative 3D likelihood algorithm was used to find the number of sources in the ROI and the morphology and spectrum parameters of each source. A circle region with a radius of  $6^\circ$ , centered at the position of W43 (RA =  $281.885^\circ$ , DEC =  $-1.942^\circ$ ), was chosen as the region of interest (ROI). In the first step, we included the sources in the LHAASO catalog [13] within  $8^\circ$  to the ROI center, except 1LHAASO J1848-0153u. The parameters are free for sources in the ROI region, the others are fixed. After a fitting process, we can get the TS value of the model, where the null hypothesis is the cosmic-ray background-only hypothesis. In each following step, an additional free source which is usually assumed to have a Gaussian morphology and a power-law spectrum was added to the ROI, and the last model whose increment of TS is larger than 25 is considered as the best-fit model. In each step, the newly added sources are placed at different initial positions for fitting to avoid local maxima.

### 3. Results

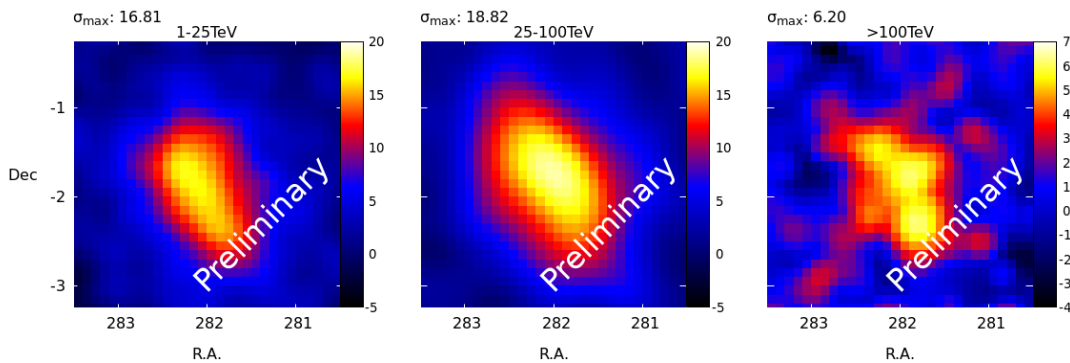


**Figure 1:** The significance maps of excess emission around the direction toward W43 direction.

To study the spatial distribution of the gamma-ray emission around W43, we picked up the sources within  $8^\circ$  to the ROI center from the LHAASO catalogue, with parameters free for sources in the ROI. And we treated all sources, with best-fit parameters, as background sources except

LHAASO J1848-0146. Then we can get a significance map about the excess mission around W43, which are shown in Fig.1. The significance of signal excess reached up to  $\sim 17\sigma$  in the energy range from 1TeV to 25TeV,  $\sim 19\sigma$  in the energy range from 25TeV to 100TeV and  $\sim 6\sigma$  in the energy range higher than 100TeV. And the morphology is quiet similar in the energy band of WCDA and the energy band of KM2A.

We used the iterative algorithm described previously to study the morphology and the spectrum of the excess emission. We discovered that a circular Gaussian distribution alone does not adequately explain the observations. Consequently, we explored alternative models, including one with two circular Gaussian sources and another with an elliptical Gaussian source. In the elliptical Gaussian model, we hypothesize the morphology of LHAASO J1848-0153u follows an elliptical Gaussian distribution, represented by:

$$\frac{dP}{d\Omega} = \frac{1}{2\pi\sigma_x\sigma_y} \exp(-a \cdot \theta_x^2 + 2b \cdot \theta_x\theta_y - c \cdot \theta_y^2) \quad (1)$$

, where

$$\begin{aligned} a &= \cos^2\theta/2\sigma_x^2 + \sin^2\theta/2\sigma_y^2 \\ b &= -\sin 2\theta/4\sigma_x^2 + \sin 2\theta/4\sigma_y^2 \\ c &= \sin^2\theta/2\sigma_x^2 + \cos^2\theta/2\sigma_y^2 \end{aligned}$$

,  $P$  is the event probability,  $\Omega$  is the solid angle,  $\theta$  is the rotation angle,  $\sigma_x$  and  $\sigma_y$  is the widths of the corresponding directions,  $\theta_x$  and  $\theta_y$  is the offsets to the center of source (R.A., Dec). The spectrum of LHAASO J1848-0153u was always assumed to be a power law  $f(E) = J \cdot (E/E_0)^\alpha$  for different morphology models.

We also added a spatial template to account for the contribution of the galactic diffuse emission. As in the first LHAASO catalog [9], the diffuse cosmic rays are assumed to be uniform, and the galactic diffuse emission is proportional to the gas column density map. The gas column density map is derived from the PLANCK dust opacity map [14, 15]. Throught out the likelihood fitting process, the spectrum of the galactic diffuse emission is assumed to be a power-law spectrum, and it was left free.

The morphology and spectral analysis is still ongoing.

#### 4. Multi-wavelength Observation

The gas distributions have been investigated in detail [16]. The total mass in the  $\gamma$ -ray emission region is estimated to be  $3 \times 10^6 M_\odot$ , and the average density is  $140 \text{ cm}^{-3}$ .

In lower energy, extended  $\gamma$ -ray emission from the W43 region has also been detected by Fermi-LAT [16]. In the GeV band, the emission is modeled as a disk with a radius of about  $0.6^\circ$ , centered at (RA=282.22°  $\pm$  0.1°, DEC=-1.65°  $\pm$  0.1°). The observed GeV radiation coincides to some extent with the TeV radiation we observed.

Besides the W43 star-forming region, additional potential astrophysical sources nearby could contribute to the gamma-ray emissions. From the ATNF pulsar catalog<sup>1</sup> [17, 18], three pulsars are

<sup>1</sup><https://www.atnf.csiro.au>

close to the region of gamma-ray emission: PSR J1847-0130, PSR J1848-0055, and PSR B1845-01. Their spin-down luminosities are  $1.7 \times 10^{32}$  ergs/s,  $2.6 \times 10^{33}$  ergs/s, and  $7.2 \times 10^{32}$  ergs/s, respectively, with distances of 5.8, 7.4, and 4.4 kpc. However, our initial evaluations indicate that these pulsars are insufficient to account for the energetic emissions here.

Several supernova remnants (SNRs) are also close the gamma-ray emission. SNR G31.5-0.6, which has an incomplete shell, is situated within the gamma-ray emission area. Its distance, estimated at 12.9 kpc using the  $\Sigma$ -D relation [19]. In the east of the gamma-ray emission area lies the mixed-morphology SNR 3C 391, aged approximately 4000 years and located 7.2 kpc away. This SNR's GeV emissions have been thoroughly investigated [20]. While it is also possible that the extensive gamma-ray emissions in the W43 region result from interactions between cosmic rays, which have escaped these SNRs, and the surrounding gas, the substantial distances of these SNRs from the dense gas in the region seem to undermine the likelihood of this scenario.

To determine the origin of the TeV gamma-ray emission we observed, further research and deeper analysis is currently ongoing.

## References

- [1] Q. Nguyen Luong, F. Motte, F. Schuller, N. Schneider, S. Bontemps, P. Schilke et al., *W43: the closest molecular complex of the Galactic bar?*, **529** (2011) A41 [1102.3460].
- [2] F. Motte, P. Schilke and D.C. Lis, *From massive protostars to a giant h ii region: Submillimeter imaging of the galactic ministarburst w43*, *The Astrophysical Journal* **582** (2003) 277.
- [3] M. Ackermann, M. Ajello, A. Allafort, L. Baldini, J. Ballet, G. Barbiellini et al., *A cocoon of freshly accelerated cosmic rays detected by fermi in the cygnus superbubble*, *Science* **334** (2011) 1103 [<https://www.science.org/doi/pdf/10.1126/science.1210311>].
- [4] H. E. S. S. Collaboration, A. Abramowski, F. Aharonian, F. Ait Benkhali, A.G. Akhperjanian, E.O. Angüner et al., *The exceptionally powerful TeV  $\gamma$ -ray emitters in the Large Magellanic Cloud*, *Science* **347** (2015) 406 [1501.06578].
- [5] A. Abramowski, F. Acero, F. Aharonian, A.G. Akhperjanian, G. Anton, A. Balzer et al., *Discovery of extended VHE  $\gamma$ -ray emission from the vicinity of the young massive stellar cluster Westerlund 1*, **537** (2012) A114 [1111.2043].
- [6] R.-Z. Yang and Y. Wang, *The diffuse gamma-ray emission toward the Galactic mini starburst W43*, **640** (2020) A60 [2007.15295].
- [7] F. Aharonian, R. Yang and E. de Oña Wilhelmi, *Massive stars as major factories of Galactic cosmic rays*, *Nature Astronomy* **3** (2019) 561.
- [8] Z. Cao, F.A. Aharonian, Q. An, L.X. Axikegu, Bai, Y.X. Bai, Y.W. Bao et al., *Ultrahigh-energy photons up to 1.4 petaelectronvolts from 12  $\gamma$ -ray Galactic sources*, **594** (2021) 33.

- [9] Z. Cao, F. Aharonian, Q. An, Axikegu, Y.X. Bai, Y.W. Bao et al., *The First LHAASO Catalog of Gamma-Ray Sources*, *arXiv e-prints* (2023) arXiv:2305.17030 [2305.17030].
- [10] F. Aharonian, V. Alekseenko, Q. An, Axikegu, L. Bai, Y. Bao et al., *Prospects for a multi-teV gamma-ray sky survey with the lhaaso water cherenkov detector array \**, *Chinese Physics C* **44** (2020) 065001.
- [11] R. Fleysher, L. Fleysher, P. Nemethy, A.I. Mincer and T.J. Haines, *Tests of statistical significance and background estimation in gamma-ray air shower experiments*, *The Astrophysical Journal* **603** (2004) 355.
- [12] S.S. Wilks, *The Large-Sample Distribution of the Likelihood Ratio for Testing Composite Hypotheses*, *The Annals of Mathematical Statistics* **9** (1938) 60 .
- [13] Z. Cao, F. Aharonian, Q. An, Axikegu, Y.X. Bai, Y.W. Bao et al., *The first lhaaso catalog of gamma-ray sources*, 2023.
- [14] Planck Collaboration, N. Aghanim, M. Ashdown, J. Aumont, C. Baccigalupi, M. Ballardini et al., *Planck intermediate results. XLVIII. Disentangling Galactic dust emission and cosmic infrared background anisotropies*, **596** (2016) A109 [1605.09387].
- [15] Planck Collaboration, A. Abergel, P.A.R. Ade, N. Aghanim, M.I.R. Alves, G. Aniano et al., *Planck 2013 results. XI. All-sky model of thermal dust emission*, **571** (2014) A11 [1312.1300].
- [16] R.-Z. Yang and Y. Wang, *The diffuse gamma-ray emission toward the Galactic mini starburst W43*, **640** (2020) A60 [2007.15295].
- [17] R.N. Manchester, G.B. Hobbs, A. Teoh and M. Hobbs, *The Australia Telescope National Facility Pulsar Catalogue*, **129** (2005) 1993 [astro-ph/0412641].
- [18] R.N. Manchester, G.B. Hobbs, A. Teoh and M. Hobbs, *The Australia Telescope National Facility Pulsar Catalogue (1.70 version)*, 2023.
- [19] G.L. Case and D. Bhattacharya, *A New  $\Sigma$ -D Relation and Its Application to the Galactic Supernova Remnant Distribution*, **504** (1998) 761 [astro-ph/9807162].
- [20] T. Ergin, A. Sezer, L. Saha, P. Majumdar, A. Chatterjee, A. Bayirli et al., *Recombining Plasma in the Gamma-Ray-emitting Mixed-morphology Supernova Remnant 3C 391*, **790** (2014) 65 [1406.2179].